Published in final edited form as:
J Neural Eng. 2009 October ; 6(5): 055009. doi:10.1088/1741-2560/6/5/055009.

Microstimulation of primary afferent neurons in the L7 dorsal root ganglia using multielectrode arrays in anesthetized cat: thresholds and recruitment properties

R.A. Gaunt[1], **J.A. Hokanson**[2], and **D.J. Weber**[1,2]

R.A. Gaunt: rag53@pitt.edu; J.A. Hokanson: jah104@pitt.edu; D.J. Weber: djw50@pitt.edu

[1] Department of Physical Medicine and Rehabilitation, 3471 Fifth Avenue, Suite 202, University of Pittsburgh, Pittsburgh, PA, 15213

[2] Department of Bioengineering, Room 5065 BST3, University of Pittsburgh, Pittsburgh, PA, 15260

Abstract

Current research in motor neural prosthetics has focused primarily on issues related to the extraction of motor command signals from the brain (e.g. brain-machine interfaces) to direct the motion of prosthetic limbs. Patients using these types systems could benefit from a somatosensory neural interface that conveys natural tactile and kinesthetic sensations for the prosthesis. Electrical microstimulation within the dorsal root ganglia (DRG) has been proposed as one method to accomplish this, yet little is known about the recruitment properties of electrical microstimulation in activating nerve fibers in this structure. Current-controlled microstimulation pulses in the range of 1–15 μA (200 μs, leading cathodic pulse) were delivered to the L7 DRG in four anesthetized cats using penetrating microelectrode arrays. Evoked responses and their corresponding conduction velocities (CVs) were measured in the sciatic nerve with a 5-pole nerve cuff electrode arranged as two adjacent tripoles. It was found that in 76% of the 69 electrodes tested, the stimulus threshold was less than or equal to 3 μA, with the lowest recorded threshold being 1.1 μA. The CVs of afferents recruited at threshold had a bimodal distribution with peaks at 70 m/s and 85 m/s. In 53% of cases, the CV of the response at threshold was slower (i.e. smaller diameter fiber) than the CVs of responses observed at increasing stimulation amplitudes. DRG microstimulation recruited afferent fibers with a range of sensory modalities (as identified by their CVs) at low stimulation intensities, and may therefore serve as an attractive location from which to introduce artificial somatosensory information into the nervous system.

1. Introduction

In recent decades the feasibility and utility of neural prostheses and functional electrical stimulation (FES) has been widely demonstrated in both animal models and humans. Brain-computer-interfaces offer the possibility of expressing motor command signals via decoded neural signals (Fetz, 1969, Hochberg et al., 2006, Schwartz et al., 2006, Velliste et al., 2008), enabling direct neural control of prosthetic limbs (Velliste et al., 2008) or control over the reanimation of paralyzed muscles in a native limb by FES (Moritz et al., 2008). Despite these successful interfaces with the motor system, there remains a need to develop a somatosensory neural interface (SSNI) that can provide the nervous system with high-dimensional artificial somatosensory feedback in a manner that could be functionally relevant for prosthetic control.

A SSNI could improve the performance and user-acceptance of a neural prosthesis, because limb-state feedback is vital for achieving stable and adaptive motor control, particularly for grasp and manipulation tasks where visual feedback alone is insufficient. Loss of somatic sensation is a major cause of disability, not only because it diminishes the ability to touch and

manipulate objects, but also because it is associated with other problems such as chronic pain and damage to hands and feet. Lacking proprioceptive feedback, patients with large-fiber sensory neuropathies exhibit severe impairments in the coordination of movements at multiple joints (Sainburg et al., 1993) and a degradation in the accuracy of movements performed without visual guidance (Sanes et al., 1984). Creating a neural interface that restores natural and complete tactile, proprioceptive, and thermal sensations will be extremely challenging, if not impossible. However, results from studies in animals (Romo et al., 1998) and humans (Dhillon and Horch, 2005) support the feasibility of providing at least some level of meaningful sensation through electrical stimulation of somatosensory neurons located at central or peripheral sites in the nervous system.

Patterned electrical stimulation of sensory neurons can be used to introduce surrogate sensory signals into the nervous system, where information is encoded in the rate, number and type(s) of sensory fibers being activated. Microstimulation studies have shown that discrete and graded tactile sensations can be evoked through stimulation at either peripheral or central locations in the nervous system. For example, microstimulation of single peripheral afferents evokes conscious sensations of flutter-vibration and pressure in humans (Vallbo, 1981, Ochoa and Torebjork, 1983, Macefield et al., 1990). Similarly, studies in humans undergoing neurosurgical treatments for tremor revealed that threshold microstimulation in the somatic sensory nucleus of the thalamus evokes sensations of touch, pressure, and body movement (Ohara et al., 2004). Primary somatosensory cortex is yet another central target for introducing somatosensory feedback as demonstrated by work in non-human primates (London et al., 2008). However, targeting first order neurons (i.e. primary afferents) may provide the most complete and natural scenario for transmitting somatosensory information, because activation of sensory neurons at the point of entry into the central nervous system ensures that the feedback is delivered to all of the central targets involved normally in sensory processing. These central targets include the cerebellar and spinal circuits that are involved in coordinating movements among multiple joints and limbs (Thach, 1998, Zehr and Duysens, 2004).

Primary afferent neurons can be accessed directly by implanting electrodes in the peripheral nerve or dorsal roots, including the dorsal root ganglia (DRG) region containing the cell bodies for these neurons. Implanting microelectrode arrays in the dorsal roots and DRG offers some advantages in that afferent fibers from an entire limb are consolidated into a few adjacent roots containing purely sensory fibers. These fibers become more distributed and mixed with efferent fibers in the peripheral nerve. Also, the roots and DRG are protected by the spinal column and are less mobile than the peripheral nerve, offering better isolation from mechanical forces that may damage or dislodge the implant. Although accessing the spinal roots requires an invasive laminectomy, the mechanical protection afforded by the surrounding vertebral bone may prove beneficial to long-term stability of the neural interface. Long term recordings of afferent fibers in the DRG have been performed (Prochazka et al., 1976, Loeb et al., 1977) and recent work shows that these signals can be decoded to predict hindlimb kinematics in the cat (Weber et al., 2007). However, the DRG has remained unexplored as a stimulation target for the development of a SSNI.

The primary aim of this paper is to characterize the recruitment of DRG neurons by single channel microstimulation applied through penetrating microelectrodes. This work provides a basic evaluation of the technical feasibility of DRG stimulation in preparation for investigation of the broader goal of using patterned multichannel microstimulation of primary afferent neurons in the DRG to transmit tactile and proprioceptive feedback to users of prosthetic limbs. The specific properties that we examined include: threshold stimulation amplitude, caliber of fibers activated at threshold and higher stimulation amplitudes, stimulation range for recruitment of responses with the same conduction velocity, and the effect of stimulation

location within the DRG. Portions of this work have been published as abstracts (Hokanson et al., 2008).

2. Methods

Acute experiments were performed in four anesthetized cats to measure the stimulation thresholds and recruitment properties of primary afferent neurons in the DRG using multichannel microstimulation. All procedures were approved by the University of Pittsburgh Institutional Animal Care and Use Committee.

2.1. Microelectrode array and nerve-cuff implant surgery

Adult cats (3–5 kg) were anesthetized with isoflurane throughout the experiment. A venous catheter was inserted into each of the forelimbs to administer fluids and drugs. At the beginning of surgery, atropine sulfate (0.15 mg/kg IV) was administered to reduce airway secretions. Blood pressure, ECG, core body temperature, oxygen saturation, and end tidal CO_2 were monitored continuously throughout the experiment. An electric heat pad and ceramic heater were used to maintain body temperature near 37° C. At the conclusion of the experiment, the animal was euthanized with a 5 mg/kg dose of potassium chloride.

A 5-pole nerve cuff electrode array was placed around the sciatic nerve midway along the thigh (distal to the bifurcation of the muscular branch, but proximal to the separation of the common personal and tibial branches) to record activity in the electroneurogram (ENG) during DRG microstimulation. The central and outermost electrodes of the sciatic nerve cuff (SNC) were connected together to act as a common reference electrode against which the active (2nd and 4th) electrodes were recorded differentially (see Figure 1C) (Hoffer et al., 1981). The active electrodes were spaced 8 mm apart. Spike-triggered averaging and stimulus-triggered averaging were used to isolate single-unit and compound action potentials in the ENG.

A laminectomy was performed to expose the spinal cord and left dorsal roots at the 6^{th} and 7^{th} lumbar segments (L6 and L7). All microstimulation was performed in the L7 DRG and some additional spike-triggered averaging data were collected in the L6 DRG. The cat was affixed in a spinal frame with the torso supported and hindlimbs extended freely. The head was fixed in a stereotaxic frame and a vertebrae clamp and hip pins were used to stabilize the spine and pelvis. Multichannel microelectrode arrays were inserted into the L6 and/or L7 DRGs. Two different array configurations were used in these experiments, but all were activated iridium microelectrodes with similar impedances of approximately 50 kΩ at 1 kHz. 16-channel “acute” arrays from NeuroNexus Technologies were used in cats #1–3 and were inserted into the L7 DRG and held in position with a micromanipulator. These arrays had 3 shanks, with 5 channels on the outer shanks and 6 on the center shank. The inter-shank spacing was 500 μm and inter-electrode spacing on each shank was 200 μm. Each electrode had a surface area of 625 μm^2. In cat #4, a pair of Cyberkinetics arrays with 400 μm interelectrode distances, a shank length of 1.5 mm, and a surface area of 2000 μm^2 per electrode were inserted into the L6 (4×10 array) and L7 (5×10 array) DRGs using a high-speed pneumatic inserter tool (Cyberkinetics, Foxborough, MA). The NeuroNexus and Cyberkinetics electrode arrays were used to access different planes of the DRG, providing a more thorough sampling of locations throughout the volume of the DRG. Figure 1 shows a diagram of the experimental setup including the electrode configurations.

2.2. Microstimulation and data acquisition protocols

An RX7 microstimulation system (Tucker-Davis Technologies, Alachua, FL) was used to deliver biphasic current pulses consisting of a leading 200 μs cathodic phase, followed by a 400 μs anodic phase of half amplitude to maintain charge balance. Reference and ground

electrodes were placed in the epidural space along the spinal cord. The stimulation intensities reported herein represent the amplitude of the cathodic phase. Stimulation pulses were delivered at 10–20 Hz to allow a high number of trials to be tested quickly. Several trials were repeated at 2 Hz yielding the same results.

In cats #1–3, stimulus intensities above and below threshold were tested repeatedly in order to resolve the threshold level to approximately 0.1 μA. Following threshold determination for cat #3, a series of stimulus intensities were tested in increasing order (3, 4, 5, 7.5, 10 and 15 μA). In cat #4, fixed stimulus intensities (1–3 μA in 0.2 μA steps, 3.5–6 μA in 0.5 μA steps, and 7–10 μA in1 μA steps) were tested in random order.

Microstimulation within the DRG elicited antidromically propagating action potentials in the sciatic nerve. These ENG signals were amplified with a gain of 10,000–20,000 and bandpass filtered (100–20,000 Hz) using a CWE BMA-400 bioamplifier (CWE Inc., Ardmore, PA). ENG signals from cats #1–3 were sampled and averaged based on the stimulus trigger using a Tektronix 3014-B oscilloscope at a frequency of 1–2.5 MHz. (Tektronix, Beaverton, OR). For cat #4, raw ENG was sampled at a rate of 300 KHz using a digital-to-analog converter (NI-USB 6259, National Instruments, Austin, TX) and stored on a computer. These data were filtered from 1–10 KHz using a 2^{nd} order Butterworth zero-phase filter, aligned each sweep to the stimulus trigger or recorded spike in the DRG, and averaged. Data sampled on the oscilloscope were also filtered using the same parameters. 500 individual sweeps were used to generate stimulus-triggered averages.

2.3. ENG analysis techniques

Stimulation-triggered averaging was used to identify neural responses in the SNC evoked by microstimulation applied through a single electrode in the DRG. The microstimulation threshold for activating neurons in the DRG was determined by finding the lowest stimulation intensity (i.e. threshold amplitude) where an identifiable response was observed in the nerve-cuff after stimulation-triggered averaging. Action potentials propagating through the cuff appear with similar shape but different latencies. Two different cross-correlation analyses were used to identify both the occurrence of activity in the SNC and the signal propagation delay between the proximal and distal electrodes in the SNC. The propagation delay was used to measure the CV of the evoked response(s) and estimate the caliber of the recruited fiber(s). These methods are described in detail in the following paragraphs.

2.3.1 Automated detection of evoked responses—An algorithm for robustly identifying the presence of one or more evoked responses in the averaged ENG was developed based on the application of a sliding-window, ‘local’ cross-correlation (LCC) analysis. LCCs were performed by selecting a 0.5 ms window (about the width of a typical waveform) from the distal of the two ENG channels and cross-correlating it with data from the proximal channel over a range of possible delays corresponding to CVs from 10–150 m/s. The maximum value for this LCC was extracted as shown in Figure 2A. The window was then moved over the entire data set for the distal channel in steps of 50 μs, generating a time-series of maximum LCC values spanning the entire sweep (bottom half of Figure 2B). The caption for Figure 2 contains additional information about this approach.

Significant responses in the ENG were determined by comparing the values in the pre- and post-stimulus LCC time series. The threshold for detecting a significant response was defined as the mean+3 standard deviations of the LCC values measured in the pre-stimulus interval (see Figure 2B). Points in the post-stimulus time interval where the LCC time series rose above the threshold were considered for further analysis (see the bottom half of Figure 2B for an example). To reduce false-positive detections, two additional criteria were applied before a response was considered significant. The criteria were: 1) the LCC time series must exceed

and remain above the threshold for at least two consecutive time points, and 2) the same time points must also exceed the threshold at the next highest stimulus amplitude. As a check of the accuracy of this algorithm, false positive detections occurred during the baseline period in just two of over 900 trials; however the noise in these two trials was abnormally high.

2.3.2 Determining conduction velocity for evoked responses—The CV for each evoked response identified in the previous analysis was determined by measuring the propagation delay (Δt) between the proximal and distal electrodes in the SNC. The propagation delay was measured by cross-correlation analysis, applied to the negative-slope regions of the averaged ENG signals on each electrode. The time lag corresponding to the peak of the cross-correlation function was taken to be the propagation delay (Δt). The CV was calculated using the following equation, $CV = d/\Delta t$, where d was the distance between the two electrodes in the SNC (d = 8 mm).

For small fibers, determining the intracuff propagation delay using cross-correlation became unreliable due the low amplitude of these slow responses and the noise in the system. We therefore categorized all responses with CVs less than 30 m/s as 'slow responses' and did not report their actual CVs. Slow responses were identified when significant activity, as measured by the LCC, occurred after a DRG-to-SNC delay appropriate for a CV of 30 m/s. Accurate determination of this cutoff latency required accurate knowledge of the DRG-to-SNC distance. This distance was found using a linear regression analysis. The known intracuff CV measurements (e.g. those obtained from large-diameter fibers) and associated DRG-to-SNC propagation delays (t) for each animal were fit to the regression model, $CV = D/t + bias + N(0,\sigma)$, where D was the DRG-to-SNC distance and $N(0, \sigma)$ was a zero mean Gaussian random variable with variance to represent noise. The bias term helped account for time delays and measurement error. Using the estimates for DRG-to-SNC distance obtained from this regression analysis, the time at which a response with a CV of 30 m/s would occur was calculated. Significant responses occurring after this calculated time are reported as 'slow' responses.

2.3.3 Spike-triggered averaging of ENG signals—Occasionally, spike-triggered averaging was used to isolate afferent responses propagating through the SNC during manual manipulation of the hindlimb. Isolated spikes recorded in the DRG were used to trigger and align ENG recordings and a modification of the previously described method was used to determine the presence of significant activity and the associated CV. For each trial, 75% of the available sweeps were selected at random and maximum LCC time series were constructed as described above. In addition, the propagation delays from the LCC analyses were also recorded. This random selection and analysis process was repeated 100 times. The set of 100 maximum LCC time series were averaged and the standard deviation of the delays at each time point were computed and normalized by the maximum. If a point in the averaged maximum LCC time series was greater than its mean+3 standard deviations and the normalized standard deviation of the delay at this time was less than 0.1, the point was considered a potential response. Eight such contiguous points were required in order for these points to be considered significant. Qualitatively this algorithm selected significant responses based on high values of the LCC and consistent estimates of the intracuff delay. This algorithm reliably detected only one response per channel, which was always at a physiologically reasonable time.

3. Results

The primary aim of this study was to characterize the recruitment of primary afferent fibers in response to electrical microstimulation applied through penetrating microelectrode arrays in the DRG of anesthetized cats. Stimulation was applied, one electrode at a time, at multiple sites in the L7 DRG via a 16-channel (cats #1–3) or 50-channel (cat #4) microelectrode array. In

cats #1 and #3, all 16 electrodes were tested while in cat #2, 5 electrodes were tested and in cat #4, 32 electrodes were tested. Evoked responses were measured in the sciatic nerve with a nerve cuff electrode.

3.1. Stimulus threshold

Across all cats, the average microstimulation threshold for detecting ENG activity in the nerve cuff was 2.7 ± 1.3 μA. The lowest stimulus amplitude that elicited a response was 1.1 μA and in 76% of the cases, the threshold stimulus amplitude was less than or equal to 3 μA. There was no significant difference ($p = 0.16$) in recruitment thresholds between the animals with the mean threshold stimulus amplitude in each animal being 2.2 ± 0.5 μA, 3.4 ± 2.3 μA, 2.6 ± 1.6 μA, and 2.9 ± 1.1 μA. Of all the electrodes, stimulation through only five electrodes failed to elicit activity in the nerve cuff up to the maximum tested stimulation amplitude. In every case where the stimulus threshold was determined, the CV of the response was also measured. In most cases, a single response was detected at the stimulus threshold. However, on 18 electrodes, responses at multiple CVs were detected at threshold. Among all responses detected at threshold, it was found that the CVs were distributed from 38 m/s to 118 m/s with the average CV at threshold across all animals being 72 ± 17 m/s.

Figure 3 summarizes these results in terms of the threshold stimulation amplitude and the CVs measured at threshold for each electrode. Figure 3A shows a scatter plot of CVs and stimulus amplitudes for all threshold responses. The scatter plot demonstrates the independence of stimulus amplitude and fiber size at threshold, as there was no significant relationship between the stimulus threshold and the CV of the fiber recruited at threshold in any animal or in the grouped data. For example, in cat #3 (‘x’ symbols in Figure 3A), one electrode had a threshold of 1.1 μA with an associated CV of 118 m/s while another electrode had a threshold of 1.3 μA and CV of 57 m/s. In cat #4 (‘◇’ symbols in Figure 3A), one electrode had a threshold of 1.2 μA and a CV of 44 m/s while another electrode had a threshold of 1.6 μA and a CV of 104 m/s.

The stacked histogram in Figure 3B shows the normalized distribution of stimulus thresholds for each animal. In this figure, the stimulation amplitude represents the lowest amplitude that generated a response in the nerve cuff. Separate peaks in the histogram were observed at approximately 2 μA and 3 μA. The presence of multiple peaks in this distribution may be a result of undersampling the stimulus amplitude range, especially in the first 3 animals where the stimulus amplitude was not incremented systematically. However, given that in these animals threshold responses were recorded at lower stimulus amplitudes on some electrodes, this is unlikely. As noted previously, the majority of the threshold responses occurred at or below 3 μA and only 2 channels had thresholds higher than 6 μA.

The stacked histogram in Figure 3C shows the normalized distribution of CVs measured at the threshold stimulus amplitude for each electrode. Two distinct peaks in the measured CVs at threshold were observed at approximately 85 m/s and 70 m/s. These correspond to the median CV of axons in the group I range (~85 m/s) and Aβ range (~72 m/s). Fibers recruited at threshold with CVs greater than the minimum CV for group I fibers (70 m/s) accounted for 50% of the responses. If this range is expanded to include fibers with CVs greater than 60 m/s, which includes the peak of the Aβ fibers, then 81% of the threshold responses were accounted for.

3.2. Multiple responses

After the threshold microstimulation amplitude was determined, the amplitude was increased incrementally to investigate the recruitment of additional afferent fibers within the DRG. It was frequently observed that stimulation at higher amplitudes recruited fibers with distinctly different CVs and latencies than the fiber or fibers recruited at threshold. In these cases,

stimulus amplitudes and CVs were determined for this secondary response. The secondary response, in general does not represent the recruitment of the second afferent, but rather the recruitment of one or more afferents having a distinctly different CV. An example of such a secondary response is shown in Figure 4 where the threshold response (CV = 63 m/s, Aβ range) occurred at an amplitude of 3 μA and a secondary response (CV = 83 m/s, group I range) occurred at an amplitude of 5.5 μA. Of the 64 electrodes where responses were recorded in the nerve cuff, 34 exhibited a pattern where the secondary response occurred at an earlier latency than the threshold response. In a further 18 electrodes the secondary response occurred at a longer latency than the threshold response and in the remaining 12 electrodes, no clear secondary response was observed up to the maximum tested stimulation amplitude.

From the perspective of implementing a somatosensory neuroprosthesis based on DRG stimulation, it is desirable to achieve selective stimulation of one or only a few afferents. Thus, the range of microstimulation amplitudes from threshold to the appearance of a secondary response is of interest and provides a measure of the range in which recruitment of similar caliber fibers occurs. Figure 5A shows a histogram of the difference in the stimulation amplitude between the threshold and secondary responses. There was an approximately uniform distribution of stimulation amplitude differences from 0–3.5 μA. Only 8% of the electrodes had differences larger than 3.5 μA, however, 48% of the electrodes tested had amplitude differences greater than 2 μA. In addition, Figure 5A includes only those electrodes where a secondary response was recorded. In an additional 12 electrodes (19% of the total number of electrodes), no secondary response was observed up to the maximum stimulation amplitude tested.

Responses with CVs below the group II and Aβ range were never observed at threshold. However, stimulation on 22 of the 69 electrodes evoked responses with CVs less than 30 m/s at stimulus amplitudes higher than the threshold amplitude. Figure 5B shows a histogram of the difference in stimulus amplitude between the threshold and that required to recruit a response with a CV < 30 m/s. Figure 5C show the distribution of the actual stimulus amplitudes required to recruit these slow fiber responses. These figures indicate that in over half the cases, a 3 μA or greater increase in simulation intensity above threshold is required to activate afferents in the group III/Aδ range.

3.3. Early small fiber recruitment

As mentioned earlier, it was frequently observed that the CV of the response at threshold was slower than the CVs of responses that appeared at higher stimulation levels. In fact, in 53% of the electrodes that evoked responses in the nerve cuff, smaller diameter fibers were recruited at a lower threshold than larger diameter fibers. Figure 4 shows an example of a channel where a slower conducting fiber was recruited before a faster conducting fiber. In this example a single response with a CV of 64 m/s was present for stimulation amplitudes from 3–5 μA. As the stimulation amplitude increased, the magnitude of the response grew, but not until 6 μA was a new response detected at a different latency. This second response had a faster CV of 83 m/s. Overall, the CVs for the initial slow responses were 69 ± 13 m/s and the CVs for the later, fast responses were 93 ± 13 m/s. The average threshold for the initial slow response was 2.9 ± 1.5 μA while the difference in the simulation amplitude between the threshold and secondary response was 1.8 ± 1.5 μA. This pattern of responses in which axon size has very little impact on recruitment order is consistent with previous reports of intrafascicular microelectrode stimulation where the small electrode-to-axon distances dominate recruitment order (Veltink et al., 1988,Veltink et al., 1989b).

3.4. Spike-triggered averaging results

Spike-triggered averaging was used to isolate the occurrence of action potentials in the nerve cuff associated with single-unit activation in the DRG. Nerve cuff responses to spike-triggered averaging were obtained for 10 neurons in 2 cats. The average peak-to-peak amplitude of the responses in these cases was 0.68 ± 0.16 μV. As a comparison, the average peak-to-peak amplitude of responses evoked by DRG stimulation at threshold was 0.69 ± 0.28 μV at threshold in the same two animals. This value was not significantly different than the spike-triggered average responses ($p = 0.72$, Wilcoxon rank sum test). Figure 6 summarizes the peak-to-peak amplitudes of the nerve cuff responses recorded under these two conditions. The amplitude of the response measured during spike-triggered averaging represents the magnitude of a single fiber response and is consistent with the magnitude of the response evoked by microstimulation at threshold.

3.5. Location effects

The use of multielectrode arrays allowed the examination of stimulus location within the DRG as a potential source of variation in the recruitment of afferent fibers. Figure 7 shows the relationship between the location of the stimulating electrode and the threshold amplitude for activating fibers in two different CV ranges. The electrodes shown in Figure 7A–C were three shank NeuroNexus probes with 16 stimulation sites distributed in the transverse plane. The electrodes used in Figure 7D and E were on a Cyberkinetics array (5×10 configuration) in which all the electrodes were at a uniform depth (~1 mm) within the DRG. Two different planes in the DRG were sampled by the two array configurations and no evidence was found for the presence of a relationship between stimulation threshold and the physical location of the electrodes. However, it was noted in several cases that electrodes that were likely located near the edge of the DRG had higher thresholds than other electrodes. For example, in Figure 7B the electrodes with the highest threshold were located at the bottom right edge of the array (medial side of the DRG) and may have been at the border or even slightly outside the DRG. Similarly in Figure 7D, several electrodes along the lateral edge of the array had high thresholds or elicited no response up to the maximum amplitude tested. Again, it is possible that these electrodes were located at the border, or perhaps even outside the DRG.

4. Discussion

The primary result from this study is that microelectrode arrays implanted in the DRG can be used to selectively stimulate small groups of afferent fibers throughout the DRG, typically at stimulation currents less than 3 μA. Prior studies investigating microstimulation thresholds in the nervous system have reported stimulus thresholds at similarly low stimulus amplitudes in the range of 0.1–5 μA (Jankowska and Roberts, 1972). More specifically, a study of intraneural microstimulation of afferent axons to examine electrically evoked sensations reported stimulus thresholds in the similarly low range of 1–2μA (Ochoa and Torebjork, 1983). In this study, the charge per phase injected at threshold was 0.6 nC/phase and increased up to 3 nC/phase at the maximum stimulation amplitude. This corresponds to a maximum charge density of 480 μC/cm^2 and 150 μC/cm^2 for the NeuroNexus and Cyberkinetics electrodes respectively. These stimulation parameters were below the safe charge per phase limits of approximately 150 nC/phase (McCreery et al., 1992) and below the charge density limits for activated iridium electrodes of approximately 1–3 mC/cm^2 (Beebe and Rose, 1988, Cogan et al., 2005).

In addition to recruiting somatosensory afferents at low thresholds, on over half of the electrodes tested, the CVs of fibers recruited at threshold were slower than the CVs of fibers recruited at subsequently higher stimulus amplitudes. Generally, recruitment of neurons by electrical stimulation is biased toward the activation of large diameter fibers at lower stimulus amplitudes than smaller diameter fibers (Durand et al., 2004). However, this large-to-small

recruitment order is primarily a concern for extraneural stimulation using cuff electrodes. Mathematical modeling (Veltink et al., 1988) and experimental work (Veltink et al., 1989a, Yoshida and Horch, 1993) demonstrate that for intraneural microelectrodes, the recruitment order is essentially neutral with no preference for either large or small diameter axons. In this study, 53% of the electrodes recruited 'slow' fibers prior to recruiting 'faster' fibers, which agrees with these previous conclusions. From the perspective of a somatosensory neural prosthesis, this pattern of recruitment is significant because it demonstrates that the location of the stimulus electrode relative to surrounding fibers within the DRG is a critical factor, and that microstimulation within the DRG is capable of selectively activating the afferent fibers for a wide range of sensory modalities.

Two results argue for the point that in many cases the responses observed at or near threshold were the result of activation of a single or just a few fibers of similar caliber. Among the 64 electrodes on which nerve cuff responses were observed, the threshold response of 46 of these electrodes contained a response at just a single CV. These CVs spanned a range that includes group I and group II muscle afferents and Aβ cutaneous fibers. If multiple axons were recruited at threshold, it is likely that the nerve cuff activity would contain responses at multiple CVs. As discussed however, this was not the observed result. Additional evidence suggesting that just a few or even a single fiber was recruited at threshold comes from the magnitude of the nerve cuff response at threshold. It was found that there was no statistical difference between the peak-to-peak amplitude of the response at threshold and the peak-to-peak amplitude of the response measured during spike-triggered averaging, which contains only the measured response to activity in a single axon. While this does not guarantee that the responses to microstimulation were also from a single fiber, our results are consistent with this possibility.

4.1. Considerations for the development of a SSNI

There are several issues that are relevant to the development of a microstimulation based SSNI. Stimulation should selectively activate one or more fibers having similar receptive fields and modalities, and increasing the intensity of stimulation should recruit additional fibers with similar properties. Also, the device should be capable of activating a wide range of sensory modalities. Previous discussion addressed the ability of microstimulation to recruit one or a small number of fibers. Our results for electrical microstimulation thresholds and recruitment within the DRG are the same as those reported for intraneural stimulation of peripheral nerve. Although microstimulation in the DRG activates a different portion of the axon than stimulation in peripheral nerve does, the sensory percepts evoked by both methods of stimulation should be similar. Intraneural stimulation has been shown to elicit very localized and finely graded responses (Dhillon and Horch, 2005), including responses of different modalities through a single electrode (Ochoa and Torebjork, 1983). It is likely that stimulation within the DRG would be similarly effective in eliciting punctate and meaningful sensations.

Stimulus amplitude modulation was used in the present study to examine changes in the peak-to-peak amplitude of the compound action potential measured in the sciatic nerve. In many cases, increases in the peak-to-peak amplitude were observed without changes in the latency or CV of the response. This suggests the recruitment of additional fibers of similar caliber and may point in some cases to localized structure in terms of axon modality within the DRG. Although the issue of somatotopy or other structural organization within the DRG is not fully understood, evidence of weak somatotopic organization exists (Burton and McFarlane, 1973, Wessels et al., 1990, Prats-Galino et al., 1999, Aoyagi et al., 2003). Furthermore, experiments in cats have shown that nerve fibers in the dorsal roots are organized in "microbundles" in which small groups of fibers from contiguous skin areas tend to run together (Wall, 1960). Such results make it plausible to achieve graded recruitment of multiple afferents having

similar modality and receptive field. Such fibers would have similar diameters, leading to the observed result.

In these experiments, it was not determined whether the receptive fields of the afferents recruited at increasing stimulus amplitudes were co-localized. Since the somatotopy of the DRG may be weak, increases in stimulus amplitude or small changes in electrode location could change the perceived stimulus location. This particular issue would be mitigated with stimulation applied in distal portions of the peripheral nerve where the fascicular organization may be stronger. The practical trade-off however is that peripheral nerve approaches would require multiple, widely distributed implant sites to cover the muscle groups and dermatomes accessible through a single DRG. In addition, the higher mobility of peripheral nerve presents a more challenging environment in which to achieve a stable, long-term interface with high-density electrode arrays.

A further necessity for a somatosensory neuroprosthetic implant is that the device should be able to activate fibers for different sensory modalities, including muscle and cutaneous afferents that subserve proprioception and tactile sensations. This seems to be possible with the present approach. Direct evidence for this comes from examination of the CVs of the responses measured at threshold. Afferents with CVs ranging from 38–118 m/s were recruited at threshold and Figure 3C shows the distribution of CVs observed at threshold. The distribution of CVs was bimodal in nature with peaks at 70 m/s and 85 m/s. This range of CVs is consistent with measurements made using spike-triggered averaging based on recordings from microelectrode arrays in the L7 ganglia (Aoyagi et al., 2003). Different CVs are closely associated with activity in specific sensory modalities. Group I, group II and Aβ axon diameter ranges along with scaling factors to convert diameter to CV (5.7 for group I and Aβ axons and 4.6 for group II axons) were used to estimate CV ranges appropriate for responses in each fiber class (Lloyd and Chang, 1948, Boyd and Kalu, 1979). Axons in these CV ranges include afferents from muscle spindles, Golgi tendon organs, and a variety of cutaneous and joint receptors (Boyd and Davey, 1968). Thus, we conclude that low intensity microstimulation through penetrating microelectrodes in the DRG is capable of activating a range of sensory modalities sufficient to elicit sensations of proprioception and touch.

A final consideration for this work, as well as all work involving the development of permanent interfaces with neural tissue is that of electrode design and stability. Chronic implants of the Cyberkinetics array in the cortex of non-human primates have shown stable recordings for 1.5 years (Suner et al., 2005), but in the DRG, stable recordings have persisted for at most several weeks (Weber et al., 2007). Arrays of individual microwires implanted in the lumbar spinal cord can maintain stable stimulation thresholds for months (Mushahwar et al., 2000). However, the development of electrode arrays suitable for implantation on the order of years is a necessary requirement before these technologies could be implemented in clinical practice.

4.2. Limitations

A potential limitation of the experimental setup concerns the presence of L7 DRG axons in the sciatic nerve, particularly in the region covered by the SNC. Proximal to the location of the nerve cuff, the sciatic nerve bifurcates and innervates the hamstrings through the muscular branch. If many of the axons in the L7 DRG do not pass through the SNC, stimulus threshold estimates could be overestimated. However, several lines of evidence suggest that this potential source of error is not likely to have significantly affected our results. First, it is known that the cutaneous afferents contained in the L7 DRG have receptive fields exclusively in the distal leg (Brown and Koerber, 1978). Second, in studies involving multielectrode recordings in the L7 DRG where unit identification was performed, very few afferents are reported as having receptive fields in regions that would not have been sampled by our nerve cuff (Aoyagi et al., 2003, Weber et al., 2006).

Examination of the data itself also suggests that this potential source of error did not substantially affect our results. Of the 69 electrodes tested, nerve cuff responses went undetected on only 5 channels over the range of stimulation amplitudes tested. This could be attributed to the afferent fibers travelling in the hamstrings nerve. Alternatively, as mentioned earlier and shown in Figure 7, these 5 electrodes were all located at the perimeter of the electrode arrays, making it plausible that the electrodes tips were not actually positioned inside the DRG. In an additional two cases, the stimulation threshold was greater than 6 μA. However, these electrodes were also located at the border of the electrode arrays. The lowest threshold measured was 1.1 μA and 76% of the electrodes had thresholds less than 3 μA. Given these points and that most of the L7 afferents travel through the sciatic nerve, it is reasonable to conclude that the sciatic nerve activity recorded at stimulation amplitudes less than 3 μA represent the activity of the first fiber recruited by DRG stimulation. Claims about the average threshold are therefore unlikely to be significantly affected by having some percentage of L7 axons not passing though the cuff. If anything, L7 fibers not passing through the nerve cuff lead to an overestimation of stimulation thresholds. This is most problematic when considering the range of stimulation amplitudes at which fibers of similar caliber are recruited (see Figure 5A). In these cases, the difference between the threshold for the first recruited response and the second recruited response could become smaller.

Another potential source of error is that stimulation within the DRG could lead to reflex activation of α-motor axons whose efferent signals would contribute to the ENG signal in the SNC. This is particularly true for the monosynaptic Ia reflex since a single primary afferent may make synaptic contact with the majority of the motoneurons within the pool (Mendell and Henneman, 1971). Nevertheless, it was felt that the low stimulation amplitudes combined with isoflurane anesthesia would be sufficient to prevent activation of spinal reflexes (Rampil and King, 1996, Zhou et al., 1997, Antognini et al., 1999). In addition, the hindlimb was monitored throughout the procedures and no movement was ever observed at the low intensities of stimulation that were tested. Finally, even had reflexes occurred, the latency at which action potentials from efferent fibers would have appeared in the nerve cuff would be noticeably later than those of afferent fibers. This point was examined by comparing the measured CVs of every identified response with the latency at which the response occurred in the SNC. Since the distance from the DRG to the SNC was known, and given a minimum additional 1 ms to account for synaptic delay and conduction to and from the spinal cord from the DRG, the latencies for expected efferent responses were calculated. For example, in cat #4, the DRG-to-SNC distance was 126 mm. For an identified response with a measured CV of 70 m/s, the latency of an efferent response would have to be at least 2.8 ms as compared to the 1.8 ms latency expected for an afferent axon. In no case did the identified responses have latencies appropriate for efferent rather than afferent activity.

Another limitation of this study is the inability to accurately measure the CVs from the SNC recordings for small diameter fibers. In spite of averaging the ENG signals approximately 500 times per stimulus amplitude, the low signal-to-noise ratio for SNC recordings limited the reliable detection of responses from the smallest fibers. Since the magnitude of the ENG signal is proportional to the size of the fiber (Gasser, 1928), slower fibers were difficult to detect. Based on the relative amplitudes of detectable responses and typical noise level, we estimate that the minimum CV detectable at thresholds similar to those found for the first response was 20 m/s. Determining recruitment properties of small fibers within the DRG is an important practical consideration in terms of the potential for eliciting the full range of sensory responses including noxious responses, but is outside the scope of the present work.

4.3. Further investigation

No obvious structure was observed in terms of recruitment thresholds within the DRG although the DRG is known to consist of an inhomogeneous distribution of cell bodies and axon bundles with uncertain somatotopic organization. Histological examination of electrode locations would provide a more solid anatomical basis for interpreting differences in the response to stimulation at certain locations. For example, several electrodes exhibited very little change in the peak-to-peak response amplitude despite a four-fold increase in the stimulus amplitude, while the response on other electrodes increased by a factor of 20 or more. These differences are likely related to the varying composition and density of fibers and cell bodies surrounding each electrode in the DRG.

Another issue to examine is whether or not there is a relationship between the type of unit recorded on a given electrode and fiber type recruited at threshold. In other words, if a particular electrode records isolated spikes from a neuron with an identified modality, receptive field and CV, does the fiber recruited at the stimulation threshold have similar properties.

4.4. Conclusion

In this study we demonstrated that stimulation within the DRG is able to recruit afferent fibers at stimulation intensities similar to those described for intraneural stimulation in the peripheral nerve. These intraneural microstimulation studies in humans demonstrated that psychophysiologically relevant sensations were evoked and that these responses were somatotopically and modality specific and had graded responses to changing stimulus parameters (Vallbo, 1981, Ochoa and Torebjork, 1983). Since stimulation in the DRG accesses these same fibers, albeit at a different location, we believe that stimulation within the DRG has the potential to provide similar subjective responses to these reports, but with an additional benefit of being able to recruit a greater range of afferent fibers with different properties at the same physical location. The DRG therefore is an attractive target site for microstimulation to introduce surrogate somatosensory information into the nervous system.

Acknowledgments

The authors would like to thank Joost Wagenaar for his contributions to hardware development. This research and development project/program was conducted by the University of Pittsburgh and is made possible by a grant that was awarded and administered by the U.S. Army Medical Research & Materiel Command's (USAMRMC), and the Telemedicine & Advanced Technology Research Center (TATRC) under Contract Number: W81XWH-07-1-0716. This work was also supported by grant number 1R01EB007749 from the National Institute of Biomedical Imaging and Bioengineering and grant number 1R21NS056136 from the National Institute of Neurological Disorders and Stroke.

References

Antognini JF, Carstens E, Buzin V. Isoflurane depresses motoneuron excitability by a direct spinal action: an F-wave study. Anesth Analg 1999;88:681–5. [PubMed: 10072028]

Aoyagi Y, Stein RB, Branner A, Pearson KG, Normann RA. Capabilities of a penetrating microelectrode array for recording single units in dorsal root ganglia of the cat. J Neurosci Methods 2003;128:9–20. [PubMed: 12948544]

Beebe X, Rose TL. Charge injection limits of activated iridium oxide electrodes with 0.2 ms pulses in bicarbonate buffered saline. IEEE Trans Biomed Eng 1988;35:494–5. [PubMed: 3397105]

Boyd, IA.; Davey, MR. Composition of peripheral nerves. Edinburgh, London: E. & S. Livingstone; 1968.

Boyd IA, Kalu KU. Scaling factor relating conduction velocity and diameter for myelinated afferent nerve fibres in the cat hind limb. J Physiol (Lond) 1979;289:277–97. [PubMed: 458657]

Brown PB, Koerber HR. Cat hindlimb tactile dermatomes determined with single-unit recordings. J Neurophysiol 1978;41:260–7. [PubMed: 650266]

Burton H, Mcfarlane JJ. The organization of the seventh lumbar spinal ganglion of the cat. J Comp Neurol 1973;149:215–32. [PubMed: 4707732]

Cogan SF, Troyk PR, Ehrlich J, Plante TD. In vitro comparison of the charge-injection limits of activated iridium oxide (AIROF) and platinum-iridium microelectrodes. IEEE Trans Biomed Eng 2005;52:1612–4. [PubMed: 16189975]

Dhillon GS, Horch KW. Direct neural sensory feedback and control of a prosthetic arm. IEEE Trans Neural Syst Rehabil Eng 2005;13:468–72. [PubMed: 16425828]

Durand DM, Yoo P, Lertmanorat Z. Neural interfacing with the peripheral nervous system. Conf Proc IEEE Eng Med Biol Soc 2004;7:5329–32. [PubMed: 17271545]

Fetz EE. Operant conditioning of cortical unit activity. Science 1969;163:955–8. [PubMed: 4974291]

Gasser HS. The relation of the shape of the action potential of nerve to conduction velocity. Am J Physiol 1928;84:699–711.

Hochberg LR, Serruya MD, Friehs GM, Mukand JA, Saleh M, Caplan aH, Branner A, Chen D, Penn RD, Donoghue JP. Neuronal ensemble control of prosthetic devices by a human with tetraplegia. Nature 2006;442:164–71. [PubMed: 16838014]

Hoffer JA, Loeb GE, Pratt CA. Single unit conduction velocities from averaged nerve cuff electrode records in freely moving cats. J Neurosci Methods 1981;4:211–25. [PubMed: 7300428]

Hokanson, JA.; Wagenaar, JBW.; Weber, DJ. Society for Neuroscience Annual Meeting. Washington, DC: 2008. Recruitment of DRG neurons by electrical microstimulation.

Jankowska E, Roberts WJ. An electrophysiological demonstration of the axonal projections of single spinal interneurones in the cat. J Physiol (Lond) 1972;222:597–622. [PubMed: 5033025]

Lloyd DP, Chang HT. Afferent fibers in muscle nerves. J Neurophysiol 1948;11:199–207. [PubMed: 18865009]

Loeb GE, Bak MJ, Duysens J. Long-term unit recording from somatosensory neurons in the spinal ganglia of the freely walking cat. Science 1977;197:1192–4. [PubMed: 897663]

London BM, Jordan LR, Jackson CR, Miller LE. Electrical stimulation of the proprioceptive cortex (area 3a) used to instruct a behaving monkey. IEEE Trans Neural Syst Rehabil Eng 2008;16:32–6. [PubMed: 18303803]

Macefield G, Gandevia SC, Burke D. Perceptual responses to microstimulation of single afferents innervating joints, muscles and skin of the human hand. J Physiol 1990;429:113–29. [PubMed: 2148951]

Mccreery DB, Agnew WF, Yuen TG, Bullara LA. Damage in peripheral nerve from continuous electrical stimulation: comparison of two stimulus waveforms. Med Biol Eng Comput 1992;30:109–14. [PubMed: 1640742]

Mendell LM, Henneman E. Terminals of single Ia fibers: location, density, and distribution within a pool of 300 homonymous motoneurons. J Neurophysiol 1971;34:171–87. [PubMed: 5540577]

Moritz CT, Perlmutter SI, Fetz EE. Direct control of paralysed muscles by cortical neurons. Nature 2008;456:639–42. [PubMed: 18923392]

Mushahwar VK, Collins DF, Prochazka A. Spinal cord microstimulation generates functional limb movements in chronically implanted cats. Exp Neurol 2000;163:422–9. [PubMed: 10833317]

Ochoa J, Torebjork E. Sensations evoked by intraneural microstimulation of single mechanoreceptor units innervating the human hand. J Physiol 1983;342:633–54. [PubMed: 6631752]

Ohara S, Weiss N, Lenz FA. Microstimulation in the region of the human thalamic principal somatic sensory nucleus evokes sensations like those of mechanical stimulation and movement. J Neurophysiol 2004;91:736–45. [PubMed: 14573561]

Prats-Galino A, Puigdellivol-Sanchez A, Ruano-Gil D, Molander C. Representations of hindlimb digits in rat dorsal root ganglia. J Comp Neurol 1999;408:137–45. [PubMed: 10331585]

Prochazka A, Westerman RA, Ziccone SP. Discharges of single hindlimb afferents in the freely moving cat. J Neurophysiol 1976;39:1090–104. [PubMed: 135821]

Rampil IJ, King BS. Volatile anesthetics depress spinal motor neurons. Anesthesiology 1996;85:129–34. [PubMed: 8694358]

Romo R, Hernandez A, Zainos A, Salinas E. Somatosensory discrimination based on cortical microstimulation. Nature 1998;392:387–90. [PubMed: 9537321]

Sainburg RL, Poizner H, Ghez C. Loss of proprioception produces deficits in interjoint coordination. J Neurophysiol 1993;70:2136–47. [PubMed: 8294975]

Sanes JN, Mauritz KH, Evarts EV, Dalakas MC, Chu A. Motor deficits in patients with large-fiber sensory neuropathy. Proc Natl Acad Sci U S A 1984;81:979–82. [PubMed: 6322181]

Schwartz, aB; Cui, XT.; Weber, DJ.; Moran, DW. Brain-controlled interfaces: movement restoration with neural prosthetics. Neuron 2006;52:205–20. [PubMed: 17015237]

Suner S, Fellows MR, Vargas-Irwin C, Nakata GK, Donoghue JP. Reliability of signals from a chronically implanted, silicon-based electrode array in non-human primate primary motor cortex. IEEE Trans Neural Syst Rehabil Eng 2005;13:524–41. [PubMed: 16425835]

Thach WT. A Role for the Cerebellum in Learning Movement Coordination. Neurobiol Learn Mem 1998;70:177–188. [PubMed: 9753595]

Vallbo, aB. Sensations evoked from the glabrous skin of the human hand by electrical stimulation of unitary mechanosensitive afferents. Brain Res 1981;215:359–63. [PubMed: 7260595]

Velliste M, Perel S, Spalding MC, Whitford aS, Schwartz aB. Cortical control of a prosthetic arm for self-feeding. Nature 2008;453:1098–101. [PubMed: 18509337]

Veltink PH, Van Alste JA, Boom HB. Simulation of intrafascicular and extraneural nerve stimulation. IEEE Trans Biomed Eng 1988;35:69–75. [PubMed: 3338814]

Veltink PH, Van Alste JA, Boom HB. Multielectrode intrafascicular and extraneural stimulation. Med Biol Eng Comput 1989a;27:19–24. [PubMed: 2779293]

Veltink PH, Van Veen BK, Struijk JJ, Holsheimer J, Boom HB. A modeling study of nerve fascicle stimulation. IEEE Trans Biomed Eng 1989b;36:683–92. [PubMed: 2744792]

Wall PD. Cord cells responding to touch, damage, and temperature of skin. J Neurophysiol 1960;23:197–210. [PubMed: 13842564]

Weber DJ, Stein RB, Everaert DG, Prochazka A. Decoding sensory feedback from firing rates of afferent ensembles recorded in cat dorsal root ganglia in normal locomotion. IEEE Trans Neural Syst Rehabil Eng 2006;14:240–3. [PubMed: 16792303]

Weber DJ, Stein RB, Everaert DG, Prochazka A. Limb-state feedback from ensembles of simultaneously recorded dorsal root ganglion neurons. J Neural Eng 2007;4:S168–80. [PubMed: 17873416]

Wessels WJ, Feirabend HK, Marani E. Evidence for a rostrocaudal organization in dorsal root ganglia during development as demonstrated by intra-uterine WGA-HRP injections into the hindlimb of rat fetuses. Brain Res Dev Brain Res 1990;54:273–81.

Yoshida K, Horch K. Reduced fatigue in electrically stimulated muscle using dual channel intrafascicular electrodes with interleaved stimulation. Ann Biomed Eng 1993;21:709–14. [PubMed: 8116921]

Zehr EP, Duysens J. Regulation of arm and leg movement during human locomotion. Neuroscientist 2004;10:347–61. [PubMed: 15271262]

Zhou HH, Mehta M, Leis aA. Spinal cord motoneuron excitability during isoflurane and nitrous oxide anesthesia. Anesthesiology 1997;86:302–7. [PubMed: 9054248]

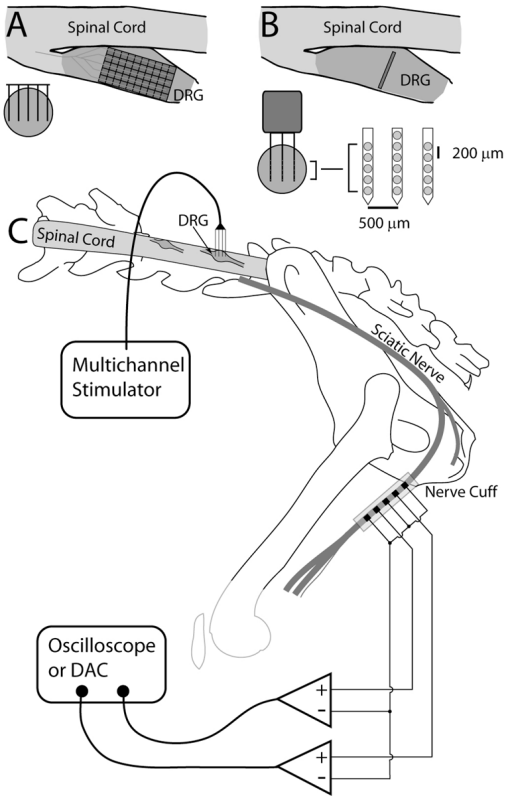

Figure 1.

Schematic of experimental setup. (A) Illustration of the insertion of individual Cyberkinetics arrays in the DRG from above (dorsal view through transverse plane, upper right) and a cross section through the DRG (lower left). (B) Illustration of the insertion of NeuroNexus probes into the DRG. The array locations shown are estimates, but the arrays were generally inserted near the center of the ganglion. C) Overall experimental setup. A multichannel recording/stimulation system was connected to the multielectrode array inserted into the DRG. A 5-pole nerve cuff was placed around the sciatic nerve and attached to a digital oscilloscope (cats #1–3) or data acquisition system (cat #4).

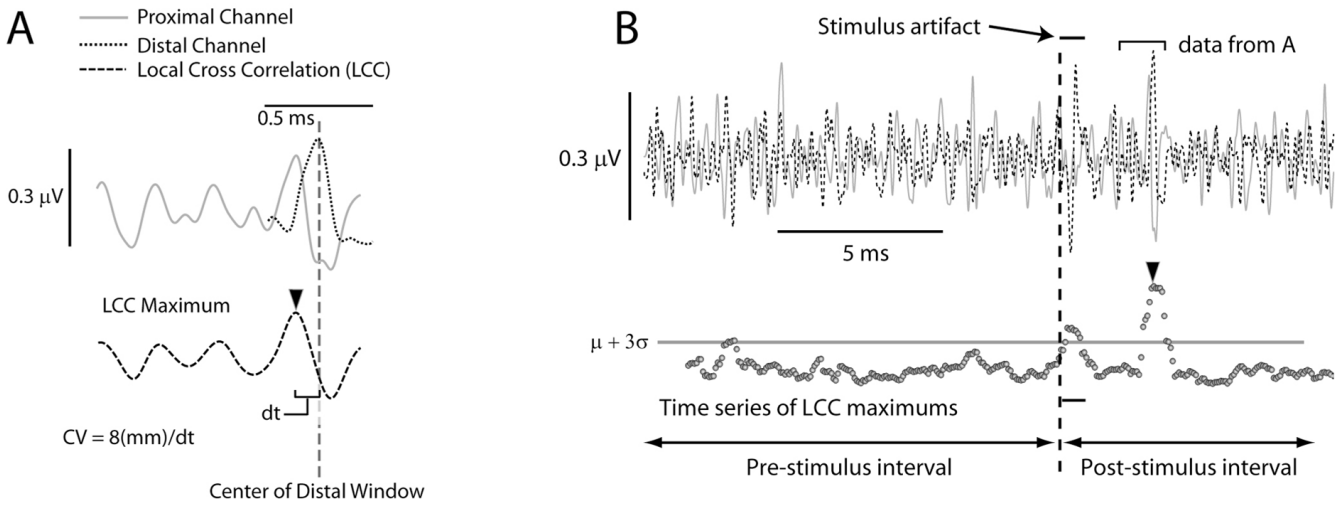

Figure 2.

Illustration of the method used to determine the first significant response in the averaged ENG recordings. (A) Example of a LCC. Data not within the appropriate local windows (see text) have been zeroed. The maximum value of the cross-correlation (arrow) is used later for determining significant responses. (B) The process was repeated for the entire sweep with the distal window shifting in 50 μs increments. Shown in the lower portion of this panel are the maximum values from the LCCs. LCC values in the pre-stimulus interval were used to calculate the mean and standard deviation of the signal.

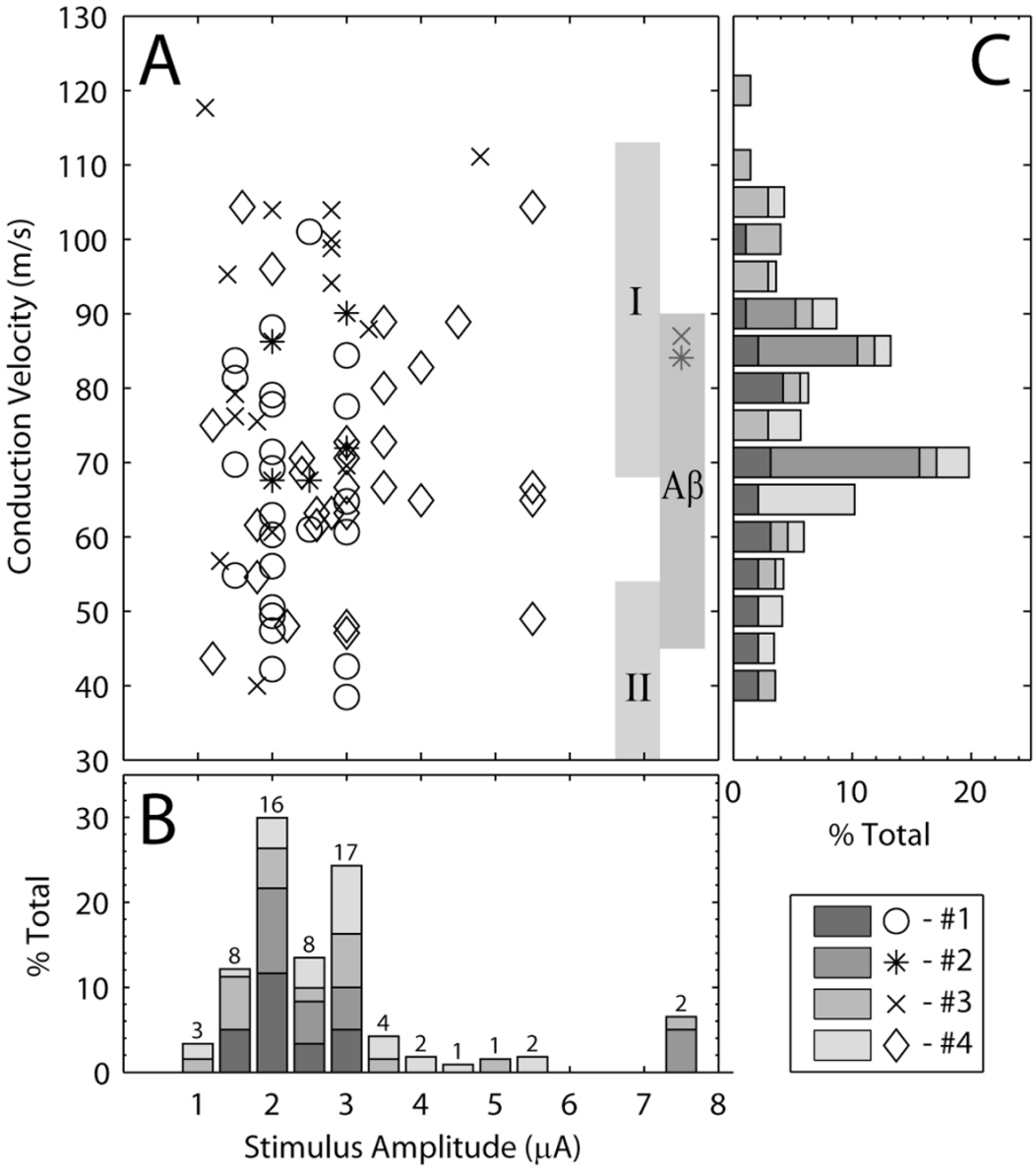

Figure 3.

Threshold stimulus amplitudes and the CV of the nerve cuff response at threshold. (A) Scatter plot of CV for evoked responses versus the corresponding stimulus amplitude. The abscissas for panels A and B are the same. The vertical gray bars in A indicate the range of CVs corresponding to group I, group II and Aβ fibers (Lloyd and Chang, 1948, Boyd and Kalu, 1979). (B) The stacked histogram shows the channel count of the stimulus amplitudes at threshold, normalized by the total count for each animal. Normalization was performed to account for the unequal numbers of electrodes tested in different animals. The total number of electrodes tested in each animal account for 25% of the total values in the histogram. The numbers above each bar indicate the number of stimulation channels in each bin. Each bar spans a 0.5 μA range centered on the value indicated below each bar. (C) Distribution of CVs for responses evoked at threshold normalized by the total count for each animal. In some cases, responses at multiple CVs were evoked at threshold, indicating recruitment of multiple fiber

types. Each bar spans a 5 m/s range centered on the value indicated to the left of each bar. The ordinates for panel C are the same as for panel A.

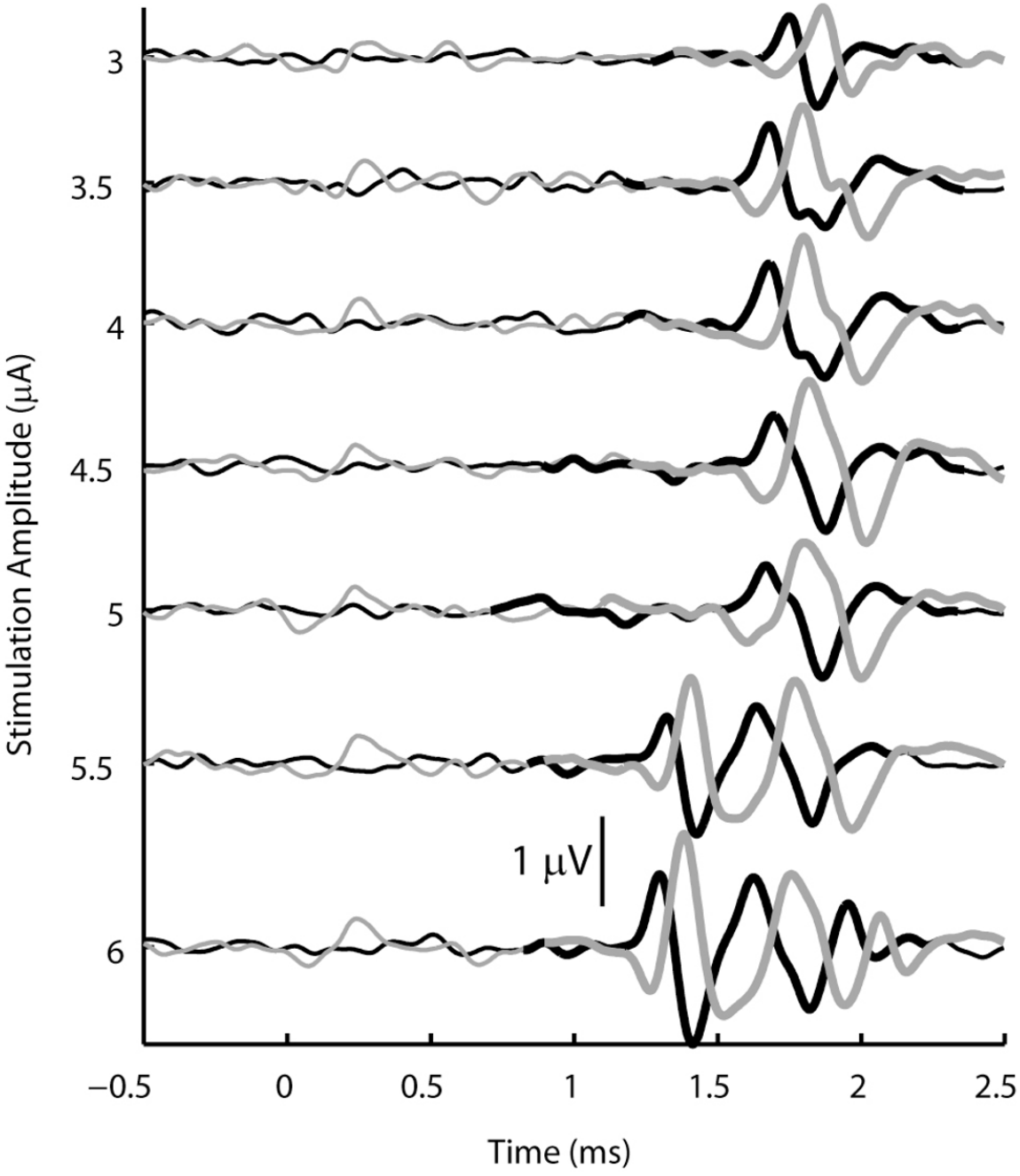

Figure 4.
Example of slow fiber recruitment prior to the recruitment of faster fibers at a higher stimulation amplitude. The CV measured at threshold was 63 m/s, and the CV of the secondary response, which first appeared at a stimulus amplitude of 5.5 μA, was 83 m/s. The signal from the proximal nerve cuff electrode is shown in black and the signal from the distal electrode is shown in gray. Thick lines indicate portions of the signal where the response was found to be significant.

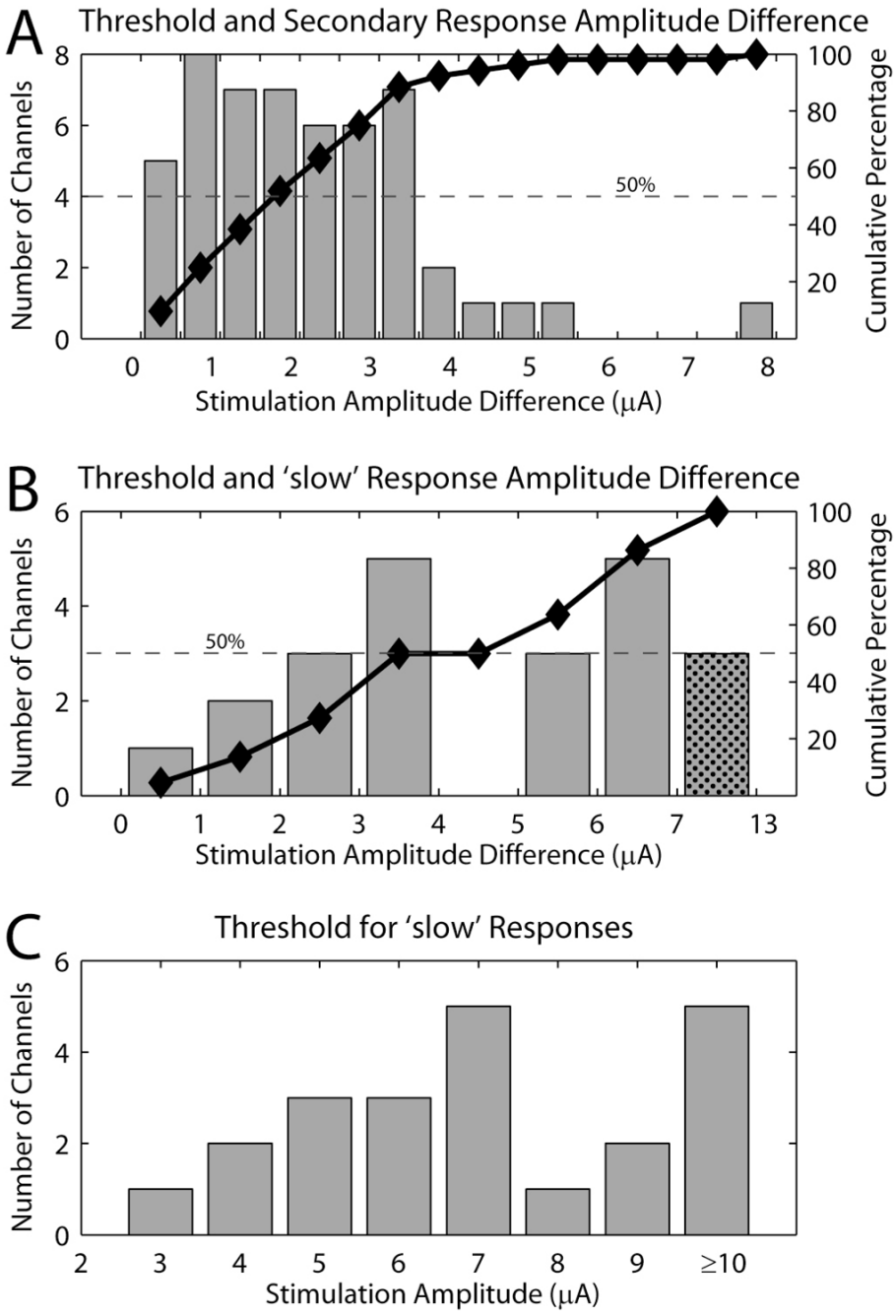

Figure 5.

Difference in stimulation amplitudes between different classes of responses. (A) Histogram of the difference in stimulus intensity at threshold and the stimulus intensity required to recruit a secondary response identified by activity at a different CV. The cumulative percentage of the distribution is plotted by the black line and markers. 100% is calculated based on the 52 electrodes that exhibited a secondary response at higher stimulus amplitudes. (B) Histogram of the difference in stimulus intensity at threshold and the stimulus intensity required to recruit a response with a CV less than 30 m/s. The smallest difference was 0.5 μA (n = 1). Significant responses with CVs less than 30 m/s were found on 22 of the 51 electrodes considered. The black line and markers show the cumulative percentage of the histogram. (C) Histogram of the

stimulus amplitude required to elicit significant responses at latencies appropriate for a CV of less than 30 m/s. 25 channels in which a response was detected showed no response from ‘slow’ fibers even at the maximum possible threshold stimulus amplitude (15 channels at 9 μA and 10 channels at 10 μA).

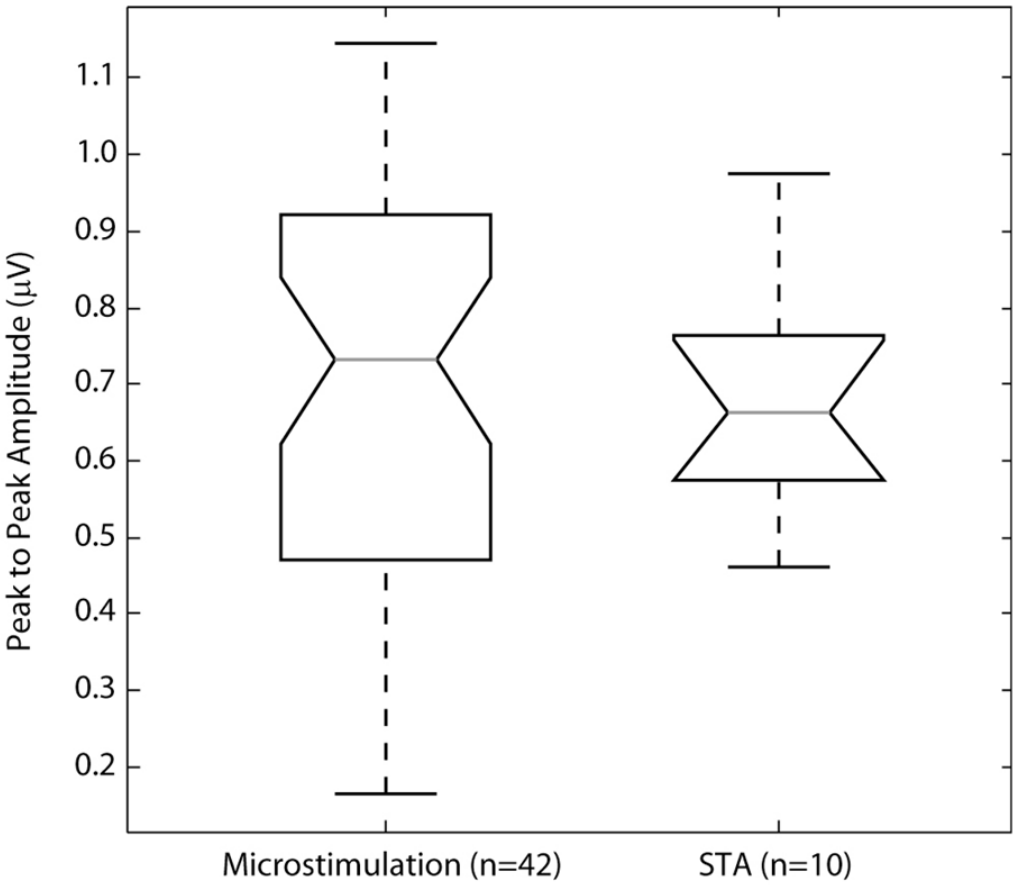

Figure 6.

Peak-to-peak response amplitudes for microstimulation trials at threshold and spike-triggered average trials in the two cats (#3 and #4) in which spike-triggered averaging trials were performed. In both cases, the mean of the proximal and distal channel were used to calculate the peak-to-peak amplitude. In cases where multiple responses were observed at the microstimulation threshold, the largest amplitude was used (n = 8 of 42 cases). The average peak-to-peak responses in the microstimulation trials and spike-triggered average trials were 0.69 ± 0.28 μV and 0.68 ± 0.16 μV respectively. No significant difference between these two groups was found (p = 0.72, Wilcoxon rank sum test). The number of trials contributing to the box plot are indicated in the abscissa labels.

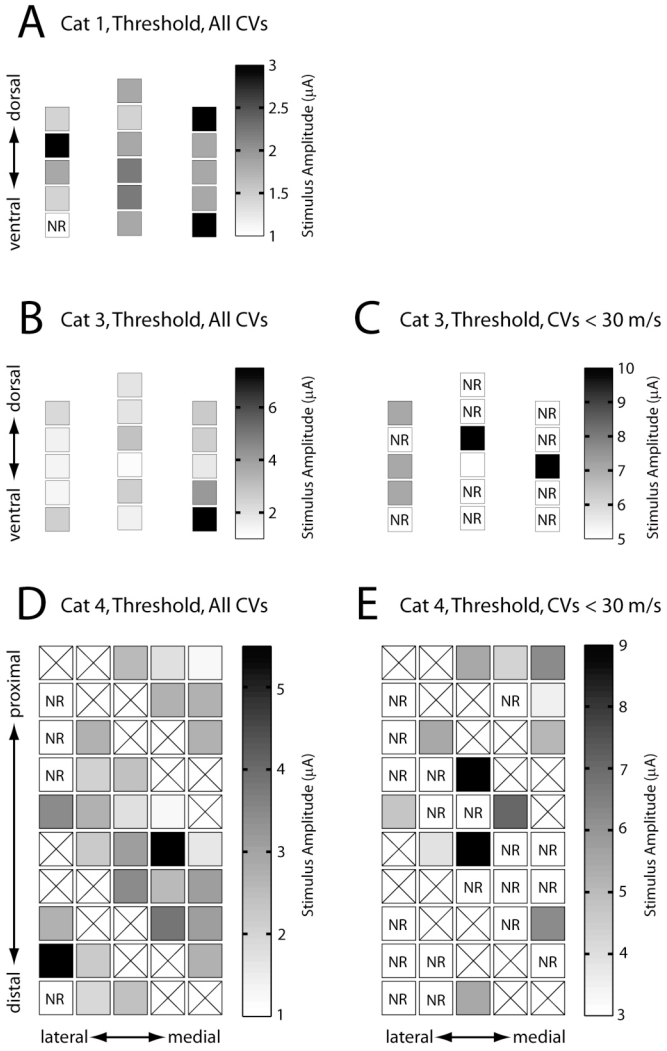

Figure 7.

Stimulus amplitude plotted by electrode location within the DRG for the threshold response in cats #1, #3, and #4 (parts A, B, and D respectively) and for the first response with a CV of less than 30 m/s in cats #3 and #4 (parts C and E respectively). Data from cat #2 was not included because only five electrodes were tested. The orientations of the electrodes within the DRG are indicated in each panel. Note that the scale bars are different for each panel. The highest thresholds shown in panel B were observed in the lower right region of the array (4.8 μA and 7.5 μA). It is possible that these electrodes were at or near the edge of the DRG perhaps accounting for their high thresholds. In addition, four electrodes on the lateral edge of the array shown in panel D did not evoke a response up to the maximum tested stimulus amplitude of 10 μA. An additional electrode on this edge had a threshold greater than 5 μA. Boxes marked with an 'X' indicate electrodes that were not tested. Boxes marked by 'NR' indicate electrodes that did not elicit a response up to the maximum tested stimulus amplitude.